Plant Science 311 (2021) 111015

Contents lists available at ScienceDirect

Plant Science

journal homepage: www.elsevier.com/locate/plantsci

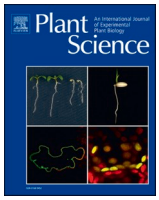

Adjustments in photosynthesis and leaf water relations are related to changes in cell wall composition in *Hordeum vulgare* and *Triticum aestivum* subjected to water deficit stress

Margalida Roig-Oliver [a,*], Mateu Fullana-Pericàs [a], Josefina Bota [a], Jaume Flexas [a,b]

[a] Research Group on Plant Biology Under Mediterranean Conditions, Departament de Biologia, Universitat de Les Illes Balears (UIB) – Agro-Environmental and Water Economics Institute (INAGEA), Carretera de Valldemossa Km 7.5, 07122, Palma, Illes Balears, Spain
[b] King Abdulaziz University, Jeddah, Saudi Arabia

ARTICLE INFO

Keywords:
Bulk modulus of elasticity
Drought
Mesophyll conductance
Monocotyledonous
Pectins
Stomatal conductance

ABSTRACT

In the current climate change scenario, understanding crops' physiological performance under water shortage is crucial to overcome drought periods. Although the implication of leaf water relations maintaining leaf turgor and stomatal functioning under water deprivation has been suggested, the relationships between photosynthesis and osmotic and elastic adjustments remain misunderstood. Similarly, only few studies in dicotyledonous analysed how changes in cell wall composition affected photosynthesis and leaf water relations under drought. To induce modifications in photosynthesis, leaf water relations and cell wall composition, *Hordeum vulgare* and *Triticum aestivum* were subjected to different water regimes: control (CL, full irrigation), moderate and severe water deficit stress (Mod WS and Sev WS, respectively). Water shortage decreased photosynthesis mainly due to stomatal conductance (g_s) declines, being accompanied by reduced osmotic potential at full turgor (π_o) and increased bulk modulus of elasticity (ε). Whereas both species enhanced pectins when intensifying water deprivation, species-dependent adjustments occurred for cellulose and hemicelluloses. From these results, we showed that π_o and ε influenced photosynthesis, particularly, g_s. Furthermore, the (Cellulose+Hemicelluloses)/Pectins ratio determined ε and mesophyll conductance (g_m) in grasses, presenting the lowest pectins content within angiosperms. Thus, we highlight the relevance of cell wall composition regulating grasses physiology during drought acclimation.

1. Introduction

Wheat (*Triticum aestivum* L.) and barley (*Hordeum vulgare* L.) are two of the most important grass crops worldwide, whose cultivars have been traditionally selected to enhance their production while increasing their drought tolerance [1–3]. In fact, water deprivation is one of the most relevant abiotic conditions limiting crops production in a climate change scenario, which is characterized by large variations in rainfalls amount, frequency, and duration [4–6]. Thus, one of the major challenges of plant physiology is to improve crops yield identifying those traits that can contribute to improve their drought tolerance [7–9]. Since photosynthesis is a crucial process influencing plants growth and productivity, it is important to understand how distinct levels of water deficit stress impose a limitation to photosynthesis performance [10–13]. Therefore, it has been described that severe water deficit stress imposition leads to important biochemical limitations to photosynthesis [11,14], whereas moderate levels of water shortage induce diffusional limitations [11, 13]. Specifically, reductions in net CO_2 assimilation (A_N) are caused by

Abbreviations: a_f, apoplastic water fraction; AIR, alcohol insoluble residue; A_N, net CO_2 assimilation; C^*_{ft}, leaf area specific capacitance at full turgor; ε, bulk modulus of elasticity; *ETR*, electron transport rate; FC, field capacity; Ψ_{md}, midday water potential; Ψ_{pd}, pre-dawn water potential; Ψ_{tlp}, water potential at turgor loss point; g_m, mesophyll conductance; g_s, stomatal conductance; LD, leaf density; LMA, leaf mass per area; PPFD, photosynthetic photon flux density; π_o, osmotic potential at full turgor; R_{light}, light respiration; RWC, leaf relative water content; RWC_{tlp}, relative water content at turgor loss point; SWC, soil water content; WUE_i, intrinsic water use efficiency.

* Corresponding author at: Margalida Roig-Oliver. Edifici Guillem Colom Casasnovas, Universitat de les Illes Balears (UIB), Carretera de Valldemossa Km 7.5, 07122, Palma, Illes Balears, Spain.
E-mail addresses: margaroig93@gmail.com (M. Roig-Oliver), mateufullana@gmail.com (M. Fullana-Pericàs), j.bota@uib.es (J. Bota), jaume.flexas@uib.es (J. Flexas).

https://doi.org/10.1016/j.plantsci.2021.111015
Received 30 April 2021; Received in revised form 28 July 2021; Accepted 3 August 2021
Available online 5 August 2021

diminishing in both stomatal and mesophyll conductances (g_s and g_m, respectively) [10–14], promoting an enhancement of the intrinsic water use efficiency (WUE_i) due to often larger declines in g_s than in g_m [15,16].

Photosynthesis performance may be related to leaf water relations under water deficit stress conditions [17]. Thus, pressure-volume (*P–V*) derived parameters –particularly, the water potential at turgor loss point (Ψ_{tlp}), the osmotic potential at full turgor (π_o), the bulk modulus of elasticity (ε) and the leaf capacitance– have been linked with photosynthesis across species [17–19]. Although modifications in both osmotic and elastic adjustments (i.e., changes in π_o and ε) have been proposed as mechanisms to face water deficit stress, their relationship with photosynthetic adjustments is still poorly understood. Hence, whereas an osmotic adjustment consisting in π_o reductions is a common response in those species submitted to water shortage [20–25], elastic adjustments could be species-specific and may involve different strategies [20,25–29]. Nevertheless, Sack et al. [30] and Niinemets [31] proposed that foliar traits –specifically, the leaf mass per area (LMA) and the leaf density (LD)– could determine ε. However, Moore et al. [32], Solecka et al. [33], Álvarez-Arenas et al. [34], Miranda-Apodaca et al. [35], Nadal et al. [18] and Roig-Oliver et al. [27,28] suggested that modifications in cell wall composition could be also important to regulate ε, but empirical evidences are for now restricted only to Roig-Oliver et al. [27].

The cell wall is a complex structure surrounding plant cells that is mainly composed of cellulose, hemicelluloses and pectins [36–40]. Of the previous, cellulose is the most abundant polysaccharide and conforms a microfibril matrix that provides mechanical strength to the wall [37–40]. Within those closely packed cellulose microfibrils, non-cellulosic polysaccharides (hereafter "hemicelluloses") are placed [36,37]. The resulting cellulose-hemicelluloses network is embedded in a pectin matrix containing cross-linking structural proteins [38,37–40], which is thought to be a relevant structure to maintain an appropriated cell wall hydric status, especially during water shortage [32,39,41,42]. Furthermore, changes in the amounts of pectins are also linked to photosynthesis –particularly, via g_m adjustments– in *Nicotiana sylvestris* and to ε in *Vitis vinifera* subjected to contrasting abiotic stressors including water deprivation [27,43]. Nonetheless, the relationships between changes in photosynthesis and leaf water relations derived parameters with modifications in cell wall composition seem to be complex and, perhaps, species-specific. In this sense, different patterns to adjust cell wall composition, leaf water relations and photosynthesis were found in *Ginkgo biloba* and *Helianthus annuus* subjected to water deficit stress [28]. Moreover, g_m was linked to lignins and cell wall bound phenolics in *H. annuus* submitted to contrasting water regimes, but instead no correlation between any cell wall compound and ε was observed [29].

To the best of our knowledge, studies focusing on the interactions between cell wall composition and changes in photosynthesis and leaf water relations parameters due to water deficit stress have been only performed in dicotyledonous species [27,29], with the exception of a dicotyledonous-gymnosperm comparison [28]. However, some of the most economically important crops worldwide are monocotyledonous and, particularly, grasses like maize, rice, sorghum, sugarcane, wheat, bamboo, oat, and barley [44,45]. In fact, monocotyledonous possess a specific cell wall composition within angiosperms as they may contain even larger proportions of cellulose and hemicelluloses –with changes in their cross-linking interactions as well as in the relative abundance of specific non-cellulosic polysaccharides–, but with a significant reduction of pectins [36,37,40,46–48]. Additionally, grasses represent a specific group within monocotyledonous from a cell wall compositional perspective because they also accumulate large quantities of mixed-linked glucans [36,37], which alterations were shown to affect g_m in mutant rice genotypes [49]. Thus, we evaluated *H. vulgare* and *T. aestivum* subjected to distinct levels of water deficit stress to detect potential relationships between changes in cell wall composition and adjustments in photosynthesis and in leaf water relations derived parameters, being g_s, g_m, π_o and ε key traits. The main hypothesis of the present study is that cell wall composition rearrangement due to water deprivation is linked to modifications in both photosynthetic and leaf water related parameters, which may have important implications for understanding grass crops physiology and management in a climate change scenario.

2. Materials and methods

2.1. Plant material, growth conditions and treatments application

T. aestivum and *H. vulgare* seeds were sown in 3 L pots containing a substrate mixture of peat and perlite (3:1, v/v) irrigated with distilled water to 100 % field capacity (FC), representing the soil moisture after the drainage of the water contained in macropores by the action of gravity. For each species, 15 individual replicates were sown. All plants were placed in a growth chamber at 25 °C and 65 % relative humidity, receiving 300 μmol m^{-2} s^{-1} photosynthetic photon flux density (PPFD) for 12 h followed by 12 h of darkness. Plants were monitored every two days weighing the pots to be watered with distilled water to 100 % FC by replacing evapo-transpired water, receiving Hoagland's solution 50 % once a week. The irrigation was manually performed. Three weeks after the sowing, three different treatments were imposed: control (CL, full irrigation), moderate water deficit stress (Mod WS; 30 % soil water content) and severe water deficit stress (Sev WS; 15 % soil water content). Five individual replicates per species were randomly subjected to each treatment. At this moment, the monitoring was daily performed to check in more detail the speed of water losses in those plants subjected to water deficit stress. The water supply in Mod WS and Sev WS treatments was stopped until reaching a specific soil water content (SWC), which was estimated as:

$$\text{SWC}\ (\%) = \frac{(\text{pot weight} - \text{minimum pot weight})}{(\text{maximum pot weight} - \text{minimum pot weight})}\ \text{x}\ 100$$

The minimum pot weight was determined placing the pots' substrate in an open-drying chamber at 70 °C for 4 days, when constant weight was reached. For each species and treatment, 4 pots were used. The maximum pot weight represented the weight of each pot when watered to 100 % FC. Finally, the pot weight corresponded to that which was daily monitored. In order to make sure that the drought treatments imposed similar adjustments in all replicates of the same species, light-saturated mid-morning stomatal conductance (g_s) was also daily monitored to check its declines in comparison to each CL treatment.– Regardless of the species, plants belonging to Mod WS reached 30 % SWC and similar g_s declines after 6 days of water shortage application. In the case of Sev WS, it took 9 days to achieve 15 % SWC and similar g_s reductions. Thus, when a desired SWC was achieved, pots' weight was noted down to be kept by adding evapo-transpired water. In all cases, treatments lasted three weeks.

2.2. Plants water status and foliar structure

At the end of the imposition of each treatment, measurements of pre-dawn (Ψ_{pd}) and midday (Ψ_{md}) leaf water potentials were performed in all plants using a pressure chamber (Model 600D; PMS Instrument Company, Albany, OR, USA). In all cases, one leaf per plant was used. Additionally, in the same leaves used for Ψ_{md}, the leaf relative water content (RWC), the leaf mass per area (LMA) and the leaf density (LD) were determined. RWC was calculated as:

$$\text{RWC}\ (\%) = \frac{\text{FW} - \text{DW}}{\text{TW} - \text{DW}}\ \text{x}\ 100$$

Where FW, DW and TW correspond to fresh, dry, and turgid weights, respectively. The FW was determined immediately after measuring Ψ_{md}.

Then, leaves were rehydrated in distilled water for 24 h under darkness conditions at 4 °C to obtain the TW. At this moment, leaves were photographed to calculate their area using ImageJ (Wayne Rasband/NIH). Also, their thickness was measured with a digital caliper from five measurements per leaf avoiding main veins. Finally, leaves were placed in an oven at 70 °C for 72 h to determine their DW. LMA was calculated as the ratio of dry weight to leaf area, while LD was estimated as thickness per area.

2.3. Gas exchange and fluorescence measurements

At the end of treatments' application, an infrared gas analyser (IRGA) LI-6400XTR coupled with a fluorometer (Li-6400−40; Li-Cor Inc., Lincoln, NE, USA) was used for simultaneous gas exchange and chlorophyll *a* fluorescence (Chl *a*) measurements. In all cases, measurements were performed from 1 h after the start of the photoperiod in the growth chamber (i.e., from 9:00 h) to 14:00 h. The block temperature, the vapour pressure deficit (VPD) and the flow rate were fixed at 25 °C, 1.5 kPa and 300 μmol min^{-1}, respectively. Per each plant, one fully developed leaf was clamped into a 2 cm^2 cuvette and steady-state conditions were induced at saturating photosynthetic photon flux density (PPFD 1500 μmol m^{-2} s^{-1}, 90–10 % red-blue light) and 400 μmol CO_2 mol^{-1} air. When steady-state conditions were reached –usually after 15–20 min–, measurements for net CO_2 assimilation (A_N), stomatal conductance (g_s), CO_2 concentration at the sub-stomatal cavity (C_i) and steady-state fluorescence (F_s) were registered. Afterward, a saturating light flash of around 8000 μmol m^{-2} s^{-1} was applied to obtain the maximum fluorescence (F_m'). From these values, the real quantum efficiency of photosystem II (Φ_{PSII}) was recorded in the equipment as follows:

$$\Phi_{PSII} = \frac{F_{m'} - F_s}{F_{m'}}$$

Moreover, light curves under non-photorespiratory conditions (< 1% O_2) were performed to estimate the electron transport rate (*ETR*) following Valentini et al. [50]. Light respiration (R_{light}) was considered as half the dark-adapted respiration rate after plants exposition to darkness for, at least, 30 min [51]. As leaves did not cover the whole area of the IRGA cuvette, a picture of the leaf fraction enclosed in the cuvette was taken to recalculate the area with ImageJ. With all previous parameters, mesophyll conductance (g_m) was calculated as described in Harley et al. [52]. Species-specific values for the CO_2 compensation point in the absence of respiration (Γ^*) were obtained from Hermida-Carrera et al. [53].

2.4. Pressure-volume curves

Per each plant, one fully developed leaf adjacent to that employed for gas exchange measurements was used to perform pressure-volume (*P–V*) curves at the end of treatments' application. Hence, leaves were rehydrated in distilled water and kept under darkness conditions overnight. The next day, leaves water potential was measured with a pressure chamber (Model 600D; PMS Instrument Company) and they were subsequently weighed to determine their fresh weight. Thus, in most cases, from complete and well-defined *P–V* curves containing 15–17 points, the leaf water potential at turgor loss point (Ψ_{tlp}), the relative water content at turgor loss point (RWC_{tlp}), the leaf osmotic potential at full turgor (π_o), the bulk modulus of elasticity (ε), the apoplastic water fraction (a_f), and the leaf area specific capacitance at full turgor (C^*_{ft}) were calculated [30,54].

2.5. Cell wall composition characterization

Those leaves used for gas exchange measurements were kept under darkness conditions overnight to minimize starch content. The next morning, sampling for cell wall composition analyses was performed in each plant. Around 500 mg of fresh leaf tissue per plant were cut in small pieces to be boiled until bleached in screwed-capped tubes containing absolute ethanol. They were cleaned twice with acetone >95 % obtaining the alcohol insoluble (AIR), an approximation of the total isolated cell wall material. AIRs were dried at room temperature and then, an α-amylase digestion was performed to eliminate starch residues. Afterward, 3 analytical replicates per AIR weighing 3 mg, approximately, were hydrolysed with 2 M trifluoroacetic acid at 121 °C for 1 h. After that, they were centrifuged obtaining two phases: a supernatant (non-cellulosic cell wall components) and a pellet (cellulosic cell wall components). Whilst non-cellulosic cell wall components were used for hemicelluloses and pectins quantifications, the pellet was cleaned twice with distilled water and acetone >95 %. The dry residue corresponding to cellulose was hydrolysed with 200 μL sulphuric acid 72 % (w/v) for 1 h, diluted to 6 mL with distilled water and heated at 121 °C until degradation. Both cellulose and hemicelluloses quantifications were performed by the phenol-sulphuric acid colorimetric procedure [55]. Hence, samples absorbance was read at 490 nm and both sugars contents were estimated interpolating samples values from a glucose calibration curve. For pectins quantification, the colorimetric method described in Blumenkrantz and Asboe-Hansen [56] was addressed using 2-hydroxybiphenil as a reagent. Thus, samples absorbance was read at 520 nm and pectins content was determined interpolating samples values from a galacturonic acid calibration curve. For all analyses, a Multiskan Sky Microplate spectrophotometer (ThermoFisher Scientific) was employed.

2.6. Statistical analysis

Prior to performing statistical analyses, Thompson test was applied to detect and subtract outliers for all tested parameters. Then, two-way analysis of variance (ANOVA) and subsequent LSD test were performed to identify statistically significant ($P < 0.05$) "species", "treatments" and "species:treatments" effects. Furthermore, Pearson's correlation matrices were done to find correlations between all studied parameters, which were considered as significant and highly significant when $P < 0.05$ and $P < 0.01$, respectively. Finally, linear regressions between photosynthetic, leaf water relations and cell wall composition parameters were fitted using mean values per species and treatment. In all cases, the R statistical software (ver. 3.2.2; R Core Team, Vienna, Austria) was employed.

3. Results

3.1. Plants water status

For both species, the reduction in water availability in Mod WS and Sev WS treatments resulted in significant declines in plant water status

Table 1
Water status of *H. vulgare* and *T. aestivum* plants subjected to different conditions (CL, control; Mod WS, moderate water deficit stress; Sev WS, severe water deficit stress). Mean values ± SE are shown for pre-dawn leaf water potential (Ψ_{pd}), midday leaf water potential (Ψ_{md}) and RWC (leaf relative water content). Species and treatments effects were quantified by two-way ANOVA and differences between groups were addressed by LSD test. *P*-values are shown. n = 5 in all cases.

Species and treatments	Ψ_{pd} (MPa)	Ψ_{md} (MPa)	RWC (%)
H. vulgare – CL	-0.23 ± 0.01^{a}	-0.82 ± 0.04^{a}	90.62 ± 2.47^{a}
H. vulgare – Mod WS	-0.50 ± 0.09^{b}	-1.30 ± 0.09^{b}	88.39 ± 1.01^{ab}
H. vulgare – Sev WS	-1.80 ± 0.05^{c}	-2.15 ± 0.04^{c}	81.81 ± 2.39^{b}
T. aestivum – CL	-0.21 ± 0.03^{a}	-0.74 ± 0.08^{a}	94.15 ± 0.72^{a}
T. aestivum – Mod WS	-0.37 ± 0.01^{ab}	-1.40 ± 0.09^{b}	88.68 ± 0.31^{ab}
T. aestivum – Sev WS	-2.07 ± 0.11^{d}	-2.66 ± 0.16^{d}	67.44 ± 4.12^{c}
Species	0.369	0.023	0.046
Treatments	<0.001	<0.001	<0.001
Species:Treatments	0.012	0.018	0.002

parameters (Table 1). Thus, both species presented more negative values for Ψ_{pd} and Ψ_{md} relative to CL, *T. aestivum* being the species achieving the lowest values (Table 1). However, both species almost maintained RWC to CL values under Mod WS, but significant reductions were found under Sev WS, being more accentuated in *T. aestivum* (Table 1).

3.2. Photosynthetic characterization

Under CL conditions, both species presented similar A_N rates (25.92 ± 1.72 and 23.87 ± 1.18 μmol CO_2 m^{-2} s^{-1} for *H. vulgare* and *T. aestivum*, respectively), which were largely reduced due to Sev WS imposition (Fig. 1A). The same pattern was also found for g_s, presenting reductions of almost 90 % and 80 % in *H. vulgare* and *T. aestivum*, respectively (Fig. 1B). Because g_s was more reduced than A_N, WUE_i was significantly higher under water deficit stress conditions than under CL in both species, especially in Sev WS treatment (107.50 ± 5.08 and 93.75 ± 9.80 μmol CO_2 mol^{-1} H_2O for *H. vulgare* and *T. aestivum*, respectively; Fig. 1C). Although g_m only declined under Sev WS in *H. vulgare* (0.07 ± 0.02 mol CO_2 m^{-2} s^{-1}), it significantly increased under Mod WS in *T. aestivum* as compared to CL (0.40 ± 0.06 and 0.23 ± 0.04 mol CO_2 m^{-2} s^{-1}, respectively), being then reduced to 0.13 ± 0.04 mol CO_2 m^{-2} s^{-1} under Sev WS (Fig. 1D). Regarding *ETR*, both "treatment" and "species" effects were significant ($P = 0.02$ and $P < 0.001$, respectively), *H. vulgare* being the species presenting more pronounced reductions due to water deficit stress treatments (Fig. 1E). Finally, only "species" effect was significant for R_{light} as *T. aestivum* presented slightly higher values than *H. vulgare* under all tested conditions (Fig. 1F).

3.3. Leaf water relations

Regarding *P–V* curves-derived parameters, water deficit stress imposed a significant shift towards more negative Ψ_{tlp} in comparison to CL, whilst no "species" effect was detected (Fig. 2A). Again, these changes were more pronounced in *T. aestivum* as Ψ_{tlp} was significantly reduced during both water deprivation treatments imposition, whereas Ψ_{tlp} was similarly maintained to CL value in *H. vulgare* subjected to Mod WS (Fig. 2A). Nonetheless, changes in RWC_{tlp} were specifically attributed to "treatments" effect ($P < 0.001$) since water shortage promoted RWC_{tlp} increasing as compared to CL (Fig. 2B). Concerning π_o, Mod WS imposition imposition resulted in large declines in *T. aestivum*, whilst it was maintained at CL value in *H. vulgare* (Fig. 2C). Nonetheless, both species presented significant reductions under Sev WS conditions, reaching -1.34 ± 0.12 and -1.20 ± 0.26 MPa in *T. aestivum* and *H. vulgare*, respectively (Fig. 2C). Regarding ε adjustments, changes were exclusively attributed to "treatments" effect ($P < 0.001$) (Fig. 2D). Thus, under Sev WS, leaves rigidity (i.e., higher ε) was almost three times larger than under CL in both species (11.33 ± 1.40 and 29.42 ± 0.30 MPa in *T. aestivum* and 10.49 ± 1.06 and 24.97 ± 3.78 MPa in *H. vulgare* under CL and Sev WS, respectively; Fig. 2D). However, no significant changes were detected for a_f (Fig. 2E). Finally, whereas 3.5-fold decreased C^*_{ft} was found in *T. aestivum* under Sev WS as compared to CL (0.29 ± 0.12 and 0.95 ± 0.15 mol H_2O m^{-2} MPa^{-1}, respectively), it was maintained similarly to CL in *H. vulgare* (0.66 ± 0.00 and 0.78 ± 0.13 mol H_2O m^{-2} MPa^{-1}, respectively; Fig. 2F).

3.4. Leaf structure and cell wall composition

Water deficit stress treatments induced different changes in both species foliar structure and cell wall composition (Table 2). Whereas an enhancement of LMA and LD was detected under Mod WS and Sev WS conditions as compared to CL in *H. vulgare*, no differences were observed in *T. aestivum* (Table 2). Regarding cell wall composition, *H. vulgare* increased the AIR content and the amounts of hemicelluloses with no changes in cellulose under Sev WS (Table 2). Instead, *T. aestivum* presented lower cellulose and hemicelluloses contents under both water shortage treatments than under CL, with no changes in AIR (Table 2). Although pectins were gradually enhanced from CL to Mod WS in *H. vulgare*, they decreased under Mod WS in *T. aestivum* in comparison to CL (Table 2). Nonetheless, both species displayed the highest amounts of pectins under Sev WS conditions (Table 2).

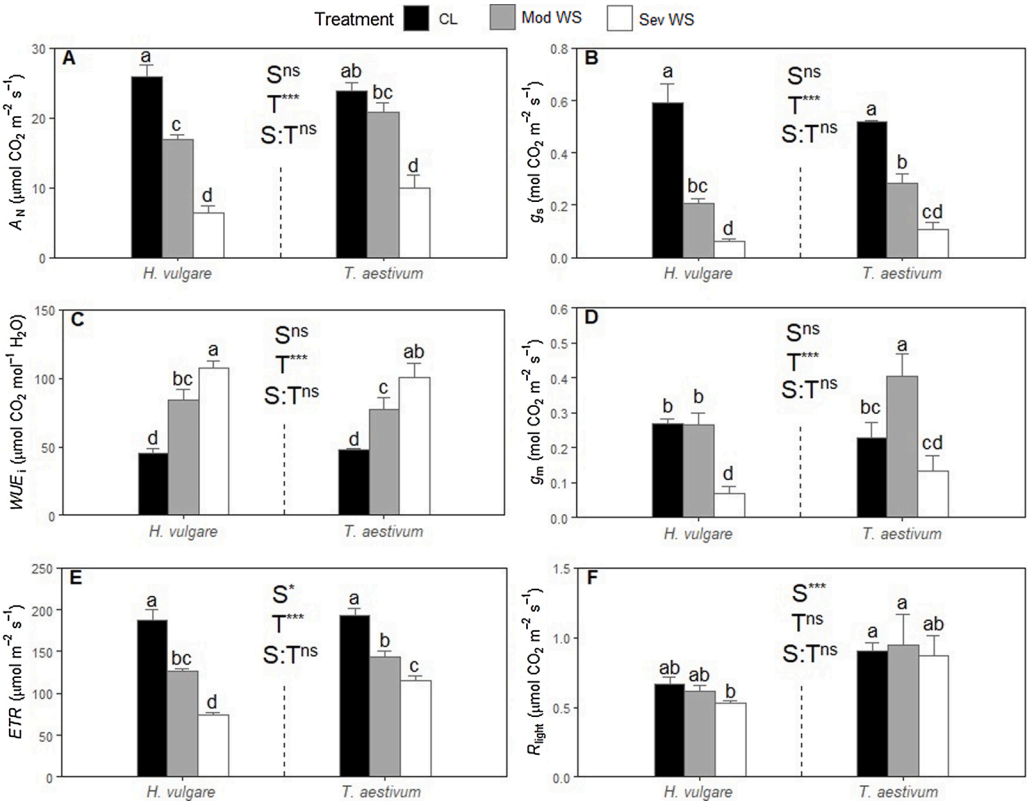

Fig. 1. Photosynthetic characterization of *H. vulgare* and *T. aestivum* plants subjected to different conditions (CL, control; Mod WS, moderate water deficit stress; Sev WS, severe water deficit stress). Saturating light conditions were applied to determine (A) net CO_2 assimilation (A_N), (B) stomatal conductance (g_s), (C) intrinsic water use efficiency (WUE_i), (D) mesophyll conductance (g_m), (E) electron transport rate (*ETR*) and (F) light respiration (R_{light}). Species (S) and treatments (T) effects were quantified by two-way ANOVA and differences between groups were addressed by LSD test. Different superscript letters indicate significant differences. Significance: *** $P < 0.001$; ** <0.01; * <0.05; ^{ns} <0.5. Values are means ± SE (n = 5).

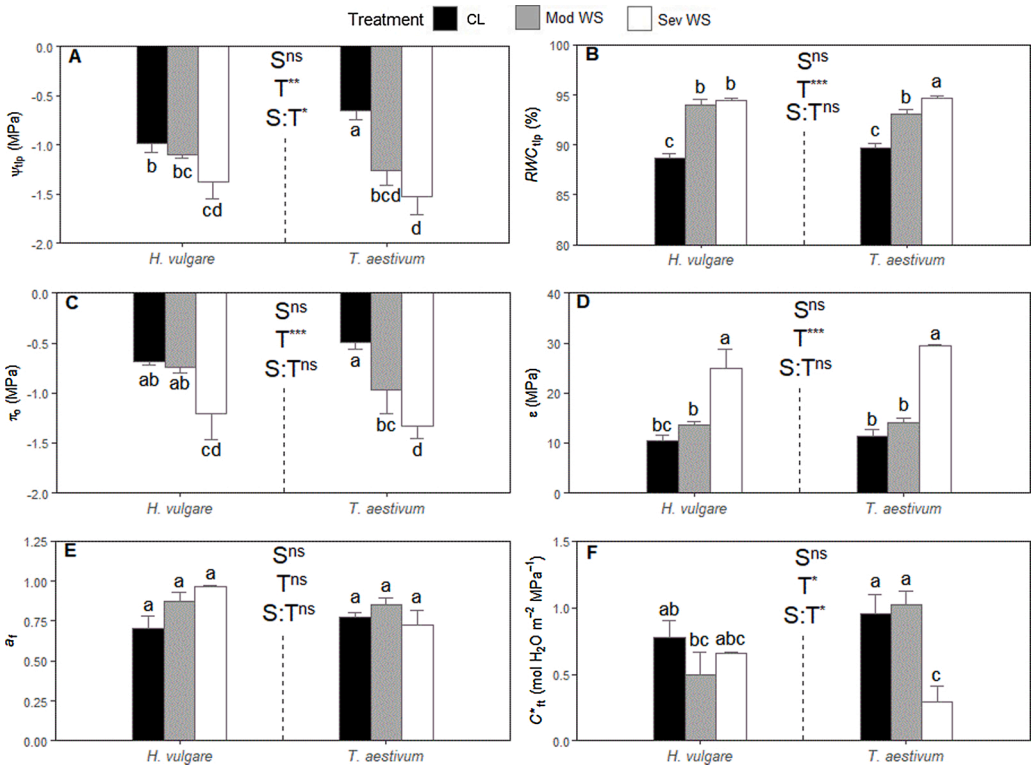

Fig. 2. Leaf water relations of *H. vulgare* and *T. aestivum* plants subjected to different conditions (CL, control; Mod WS, moderate water deficit stress; Sev WS, severe water deficit stress). (A) Water potential at turgor loss point (Ψ_{tlp}), (B) relative water content at turgor loss point (RWC_{tlp}), (C) osmotic potential at full turgor (π_o), (D) bulk modulus of elasticity (ε), (E) apoplastic water fraction (a_f), and (F) leaf area specific capacitance at full turgor (C^*_{ft}). Species (S) and treatments (T) effects were quantified by two-way ANOVA and differences between groups were addressed by LSD test. Different superscript letters indicate significant differences. Significance: *** $P < 0.001$; ** <0.01; * <0.05; ^{ns} <0.5. Values are means ± SE (n = 5).

Table 2
Leaf structural traits and cell wall composition of *H. vulgare* and *T. aestivum* plants subjected to different conditions (CL, control; Mod WS, moderate water deficit stress; Sev WS, severe water deficit stress). Mean values ± SE are shown for leaf mass per area (LMA), leaf density (LD), alcohol insoluble residue (AIR), cellulose, hemicelluloses and pectins. Species and treatments effects were quantified by two-way ANOVA and differences between groups were addressed by LSD test. Different superscript letters indicate significant differences. *P*-values are shown. n = 5 in all cases.

Species and treatments	LMA (g m^{-2})	LD (g cm^{-3})	AIR (% extracted)	Cellulose (mg g^{-1} AIR)	Hemicelluloses (mg g^{-1} AIR)	Pectins (mg g^{-1} AIR)
H. vulgare – CL	29.35 ± 0.99^{b}	0.11 ± 0.01^{b}	15.23 ± 2.47^{b}	228.99 ± 9.79^{b}	176.81 ± 15.19^{b}	26.75 ± 3.48^{c}
H. vulgare – Mod WS	40.18 ± 3.17^{a}	0.15 ± 0.02^{a}	18.72 ± 0.71^{b}	245.07 ± 12.25^{b}	179.66 ± 22.12^{b}	30.80 ± 1.15^{bc}
H. vulgare – Sev WS	41.40 ± 3.14^{a}	0.17 ± 0.01^{a}	24.88 ± 1.70^{a}	233.94 ± 4.26^{b}	229.37 ± 6.25^{a}	37.93 ± 0.52^{a}
T. aestivum – CL	41.83 ± 2.88^{a}	0.18 ± 0.01^{a}	16.41 ± 0.16^{b}	292.93 ± 3.78^{a}	227.71 ± 8.34^{a}	33.20 ± 0.77^{ab}
T. aestivum – Mod WS	38.49 ± 1.73^{a}	0.16 ± 0.01^{a}	17.38 ± 0.19^{b}	222.69 ± 12.37^{b}	207.00 ± 15.14^{ab}	29.02 ± 1.44^{bc}
T. aestivum – Sev WS	38.85 ± 1.99^{a}	0.17 ± 0.02^{a}	18.67 ± 0.79^{b}	227.08 ± 15.98^{b}	177.20 ± 15.78^{b}	36.49 ± 0.34^{a}
Species	0.292	0.023	0.075	0.214	0.607	0.326
Treatments	0.277	0.184	<0.001	0.026	0.644	<0.001
Species:Treatments	0.015	0.021	0.053	0.002	0.004	0.033

3.5. Correlations between parameters

Relationships between all studied parameters are found in Table S1. Particularly, significant negative correlations were detected between ε and the (Cellulose+Hemicelluloses)/Pectins ratio ($R^2 = 0.92$, $P < 0.01$, Fig. 3A) and g_s ($R^2 = 0.60$, $P = 0.04$, Fig. 3B). However, g_s correlated positively with π_o ($R^2 = 0.63$, $P = 0.04$, Fig. 3C) and with the (Cellulose+Hemicelluloses)/Pectins ratio ($R^2 = 0.71$, $P = 0.02$, Fig. 3D). Additionally, other significant negative correlations were found between g_m and A_N with pectins ($R^2 = 0.66$, $P = 0.03$, Fig. 4A and $R^2 = 0.67$, $P = 0.03$, Fig. 4B, respectively).

4. Discussion

In the present study, we tested two of the most relevant grass crops worldwide to examine the implications of distinct levels of water deficit stress promoting changes in their physiological performance. The classic response to water deprivation is characterized by A_N reductions due to decreasing in the overall CO_2 diffusion, resulting in enhanced WUE_i [10,14]. Although g_s declines were already detected at Mod WS in both species, g_m was similarly maintained to CL in *H. vulgare* whilst it was enhanced around 43 % in *T. aestivum* (Fig. 1B,D). In fact, enhanced g_m under water deprivation was previously reported in sunflowers subjected to long term water deficit stress [29]. Given that g_s is a reference parameter to understand plants responses to progressive drought and that severe levels of water deficit stress usually occur when g_s drops below 0.03 mol CO_2 m^{-2} s^{-1} [57], our results may indicate that the water shortage treatments we applied just imposed a moderate stress. However, the application of apparently moderate water deficit stress treatments supposed significant changes in *P–V* derived parameters (Fig. 2).

Osmotic and elastic adjustments (i.e., changes in π_o and ε) are important mechanisms to face water deprivation [20–22,24]. Although *H. vulgare* maintained π_o to CL value under Mod WS, significant declines were observed in *T. aestivum*, demonstrating that both species presented different mechanisms to face this level of water deficit stress. However, both achieved more negative π_o after their exposition to Sev WS. Nonetheless, elastic modifications were only observed under Sev WS, resulting in enlarged ε as previously reported in evergreen species subjected to drought periods [20] probably because of modifications in the foliar structure [58,59]. Since LMA and LD usually increase after plants

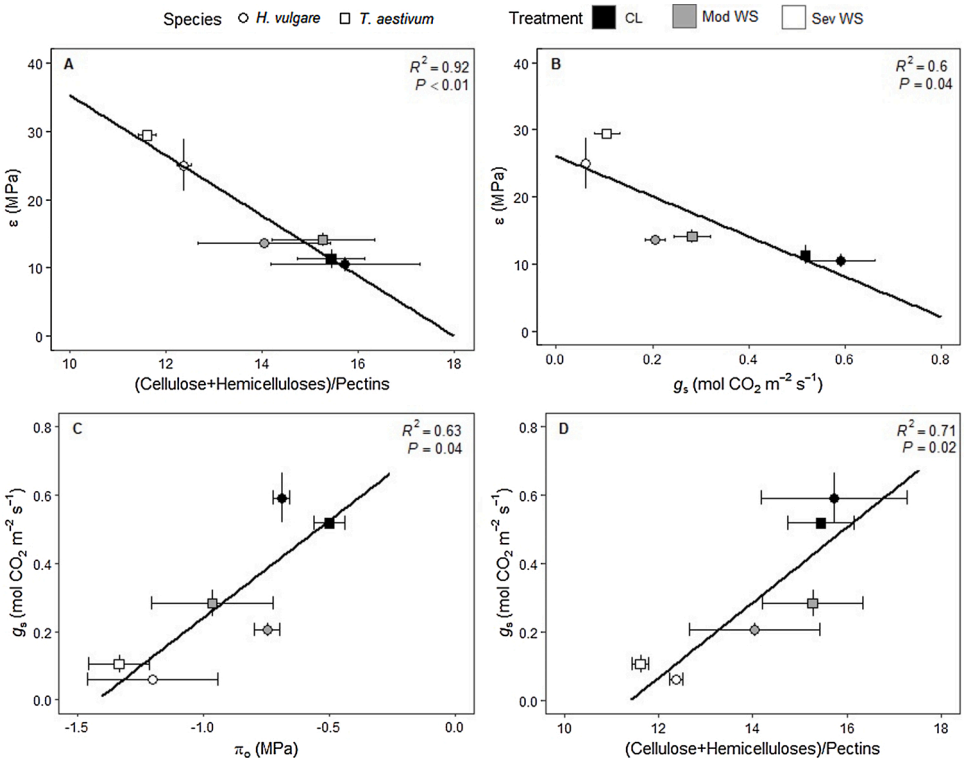

Fig. 3. Relationships between bulk modulus of elasticity (ε) and (A) (Cellulose+Hemicelluloses)/Pectins ratio and (B) stomatal conductance (g_s) and relationships between g_s and (C) osmotic potential at full turgor (π_o) and (D) (Cellulose+Hemicelluloses)/Pectins ratio in *H. vulgare* and *T. aestivum* plants subjected to different conditions (CL, control; Mod WS, moderate water deficit stress; Sev WS, severe water deficit stress). n = 5 (means ± SE).

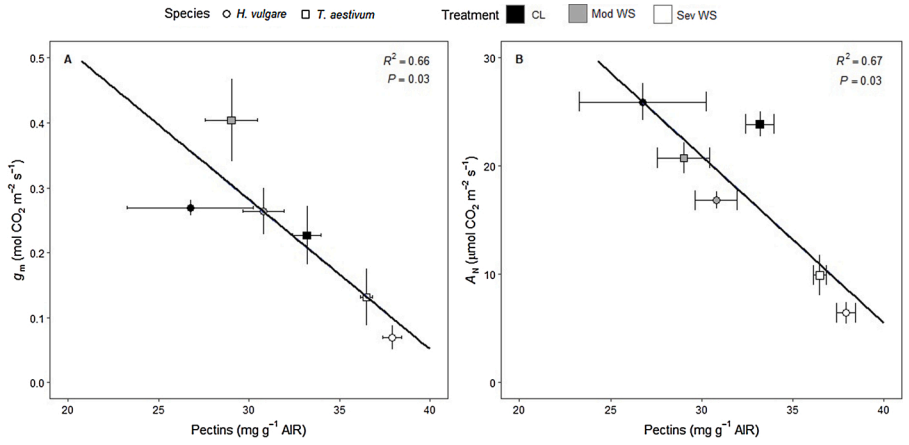

Fig. 4. (A) Relationship between mesophyll conductance (g_m) and pectins content and (B) relationship between net CO_2 assimilation (A_N) and pectins content in *H. vulgare* and *T. aestivum* plants subjected to different conditions (CL, control; Mod WS, moderate water deficit stress; Sev WS, severe water deficit stress). n = 5 (means ± SE).

exposition to water shortage, they have been correlated positively with ε across species [31,60,61]. However, in our study, the relationships between ε with LMA and LD were non-significant (Table S1), which implies that other traits were involved in ε adjustments in both grass species. Although it has been proposed that modifications in cell wall thickness may determine ε changes [62,63], it is improbable that such modifications are involved in fast ε adjustments. Thus, some studies proposed that changes in the cell wall proportion (i.e., the AIR) as well as in its compounds rearrangement may affect ε [27,32–35]. Of the previous, only Roig-Oliver et al. [27] provided empirical evidence for this, showing positive relationships between ε and AIR and pectins. In the present study, we also found that pectins content correlated with ε (Table S1), but an even more significant relationship emerged considering the (Cellulose+Hemicelluloses)/Pectins ratio (Fig. 3A), evidencing that modifications in pectins relative abundance determined elastic adjustments in grasses, even when they contain less than half pectins amounts than non-gramineous angiosperms [36,37,40,46–48]. Additionally, another two correlations between photosynthesis-related and leaf water-related parameters were further observed (Fig. 3B,C), being ε, π_o and g_s crucial traits. Lower π_o values were achieved while enhancing the level of water deprivation, being accompanied by an increasing of leaves rigidity and by declines in g_s, all of them contributing to photosynthesis reductions. Since stomatal closure was in general the main photosynthesis limitation, this study provides one of the first evidences on the relationship between g_s adjustments due to modifications in leaf cell wall composition (Fig. 3D). In fact, Gago et al. [64]

specifically proposed that changes in guard cells' cell wall composition –among other mechanisms such as specific sugars and organic acids accumulation and alterations in enzymatic processes– could influence stomatal movements, which may finally affect photosynthesis. Particularly, it has been reported that pectin arabinans degradation blocked stomatal movements in the dicotyledonous *Commelina communis* [65] and high pectins deposition were found in the guard cells' cell walls of the grass species *Zea mays* [66]. Therefore, pectins have been proposed to strongly regulate guard cells' cell wall properties [67], which may potentially affect stomata functioning and, thus, photosynthesis. Although further studies exclusively evaluating guard cells' cell wall composition are needed to confirm this role for pectins, we show that even changes in their relative proportion considering the whole leaf cell wall were also responsible of photosynthetic reductions due to g_s modulation. Also, we demonstrate pectins relevance in determining g_m and, thus, photosynthesis (Fig. 4A,B). Although Ye et al. [68] did not report any cell wall composition effect on photosynthesis testing well-watered rice genotypes, Ellsworth et al. [49] and Zhang et al. [69] analysed different rice mutants and attributed photosynthesis reductions to alterations in mixed-linked glucans and to disrupted cellulose microfibrils orientation, respectively. However, those modifications in cell wall composition affecting photosynthesis –and, particularly, g_m– under distinct abiotic stressors including water shortage have just been explored in some dicotyledonous [27,29,43] and in a dicotyledonous-gymnosperm comparison [28]. Specifically, whilst Roig-Oliver et al. [28] found distinct patterns to face water deficit stress in *G. biloba* and *H. annuus*, cellulose and pectins were exclusively linked to g_m in grapevines and tobacco, respectively [27,43]. Thus, our results are in agreement with those reported in tobacco and are of special relevance since the effect of changes in cell wall composition regulating photosynthesis –specially, g_m– in grasses remained further unexplored.

5. Conclusions

To the best our knowledge, this study provides the first evidence on the role of cell wall composition determining both photosynthesis and leaf water relations adjustments in two of the most relevant grass crops worldwide subjected to distinct water deficit stress regimes. Our results demonstrated the importance of osmotic and elastic adjustments influencing photosynthesis, being π_o, ε, and g_s key parameters. Also, we highlighted that changes in cell wall composition –particularly, in pectins content– determined leaf elasticity and both g_s and g_m. Besides these modifications in the amounts of the analysed leaf cell wall compounds, we speculate that they could be accompanied by changes in their physicochemical interactions resulting in differed guard cells movement and to altered wall porosity [65,66,70–72], which ultimately affected photosynthesis. However, the present results should be confirmed under more realistic field conditions, and further studies testing a larger number of grass crops subjected to more water shortage treatments as well as to recovery conditions are required to elucidate which physiological strategies are activated during drought events that resemble those caused by the climate change.

Author contributions

MR-O, MF-P, JB and JF conceived and designed this study; MR-O and MF-P conducted the experiment; MR-O and JF performed the data analysis and MR-O wrote the first draft of the manuscript. All authors contributed to following versions, including the final one.

Funding

This work was supported by the project PGC2018−093824-B-C41 (Ministerio de Economía y Competitividad; MINECO, Spain) and the ERDF (FEDER). MR-O and MF-P were supported by pre-doctoral fellowshipsFPU16/01544 and FPI/1929/2016 through MINECO and Govern de les Illes Balears, respectively.

Declaration of Competing Interest

The authors declare they have no potential conflict of interest.

Acknowledgements

The authors thank Mr Joan Mestre for providing the seeds of both species. Also, we thank Dr Cyril Douthe for technical support during gas exchange performance and Dr Miquel Nadal for his advices with *P-V* curves.

Appendix A. Supplementary data

Supplementary material related to this article can be found, in the online version, at doi:https://doi.org/10.1016/j.plantsci.2021.111015.

References

[1] I.K. Dawson, J. Russell, W. Powell, B. Steffenson, W.T.B. Thomas, R. Waugh, Barley: a translational model for adaptation to climate change, New Phytol. 206 (2015) 913–931.
[2] A. Sallam, A.M. Alqudah, M.F.A. Dawood, P.S. Baenziger, A. Börner, Drought stress tolerance in wheat and barley: advances in physiology, breeding and genetics research, Int. J. Mol. Sci. 20 (2019) 3137.
[3] A. Gastaldi, S. Álvarez Prado, J.A. Arduini, D.J. Miralles, Optimizing wheat (*Triticum aestivum* L.) management under dry environments: a case study in the west pampas of Argentina, Agric. Water Manag. 2333 (2020), 106092.
[4] J. Lipiec, C. Doussan, A. Nosalewicz, K. Kondracka, Effect of drought and heat stresses on plant growth and yield: a review, Int. Agrophys. 27 (2013) 463–477.
[5] R.A. Richards, J.R. Hunt, J.A. Kirkegaard, J.B. Passioura, Yield improvement and adaptation of wheat to water-limited environments in Australia - a case study, Crop Pasture Sci. 65 (2014) 676–689.
[6] V.O. Sadras, R.A. Richards, Improvement of crop yield in dry environments: benchmarks, levels of organisation and the role of nitrogen, J. Exp. Bot. 65 (2014) 1981–1995.
[7] D. Tilman, K.G. Cassman, P.A. Matson, R. Naylor, S. Polasky, Agricultural sustainability and intensive production practices, Nature 418 (2002) 671–677.
[8] J.I.L. Morison, N.R. Baker, P.M. Mullineaux, W.J. Davies, Improving water use in crop production, Philos. Trans. Biol. Sci. 363 (2008) 639–658.
[9] H.R. Schultz, Global climate change, sustainability, and some challenges for grape and wine production, J. Wine Eco. 11 (2006) 181–200.
[10] M.M. Chaves, J.P. Maroco, J.S. Pereira, Understanding plant responses to drought – from genes to the whole plant, Funct. Plant Biol. 30 (2003) 239–264.
[11] G. Grassi, F. Magnani, Stomatal, mesophyll conductance and biochemical limitations to photosynthesis as affected by drought and leaf ontogeny in ash and oak trees, Plant Cell Environ. 28 (2005) 834–849.
[12] T. Tosens, L. Laanisto, Mesophyll conductance and accurate photosynthetic carbon gain calculations, J. Exp. Bot. 69 (2018) 5315–5318.
[13] M. Nadal, J. Flexas, Variation in photosynthetic characteristics with growth form in a water-limited scenario: implications for assimilation rated and water use efficiency in crops, Agric. Water Manag. 216 (2019) 457–472.
[14] J. Flexas, J. Bota, F. Loreto, G. Cornic, T.D. Sharkey, Diffusive and metabolic limitations to photosynthesis under drought and salinity in C_3 plants, Plant Biol. 6 (2004) 269–279.
[15] J. Galmés, M.À. Conesa, J.M. Ochogavia, J.A. Perdomo, D.M. Francis, M. Ribas-Carbó, R. Savé, J. Flexas, H. Medrano, J. Cifre, Physiological and morphological adaptations in relation to water use efficiency in Mediterranean accessions of *Solanum lycopersicum*, Plant Cell Environ. 34 (2011) 245–260.
[16] J. Flexas, Ü. Niinemets, A. Gallé, M.M. Barbour, M. Centritto, A. Díaz-Espejo, C. Douthe, J. Galmés, M. Ribas-Carbó, P.L. Rodríguez, F. Rosselló, R. Soolanayakanahally, M. Tomás, I.J. Wright, G.D. Farquhar, H. Medrano, Diffusional conductances to CO_2 as a target for increasing photosynthesis and photosynthetic water-use efficiency, Photosynth. Res. 117 (2013) 45–59.
[17] D. Xiong, M. Nadal, Linking water relations and hydraulics with photosynthesis, Plant J. 101 (2020) 800–815.
[18] M. Nadal, J. Flexas, J. Gulías, Possible link between photosynthesis and leaf modulus of elasticity among vascular plants: a new player in leaf traits relationships? Ecol. Lett. 21 (2018) 1372–1379.
[19] S.D. Zhu, Y.J. Chen, Q. Ye, P.C. He, H. Liu, R.H. Li, P.L. Fu, G.F. Jiang, K.F. Cao, Leaf turgor loss point is correlated with drought tolerance and leaf carbon economics traits, Tree Physiol. 38 (2018) 658–663.
[20] M.A. Lo Gullo, S. Salleo, Different strategies of drought resistance in three Mediterranean sclerophyllous trees growing in the same environmental conditions, New Phytol. 108 (1988) 267–276.
[21] M.D. Abrams, Adaptations and responses to drought in *Quercus* species of North America, Tree Physiol. 7 (1990) 227–238.

[22] M.E. Kubiske, M.D. Abrams, Rehydration effects on pressure–volume relationships in four temperate woody species: variability with site, time of season and drought conditions, Oecologia 85 (1991) 537–542.
[23] M.K. Bartlett, C. Scoffoni, L. Sack, The determinants of leaf turgor loss point and prediction of drought tolerance of species and biomes: a global meta-analysis, Ecol. Lett. 15 (2012) 393–405.
[24] N.C. Turner, Turgor maintenance by osmotic adjustment: 40 years of progress, J. Exp. Bot. 69 (2018) 3223–3233.
[25] S. Álvarez, P. Rodríguez, F. Broetto, M.J. Sánchez-Blanco, Long term responses and adaptative strategies of *Pistacia lentiscus* under moderate and severe deficit irrigation and salinity: osmotic and elastic adjustment, growth, ion uptake and photosynthetic activity, Agr. Water Manage. 202 (2018), 253–252.
[26] M.A. Sobrado, N.C. Turner, A comparison of the water relations characteristics of *Helianthus annuus* and *Helianthus petiolaris* when subjected to water deficits, Oecologia 58 (1983) 309–313.
[27] M. Roig-Oliver, M. Nadal, M.J. Clemente-Moreno, J. Bota, J. Flexas, Cell wall components regulate photosynthesis and leaf water relations of *Vitis vinifera* cv. Grenache acclimated to contrasting environmental conditions, J. Plant Physiol. 244 (2020), 153084.
[28] M. Roig-Oliver, M. Nadal, J. Bota, J. Flexas, *Ginkgo Biloba* and *Helianthus annuus* show different strategies to adjust photosynthesis, leaf water relations, and cell wall composition under water deficit stress, Photosynthetica 58 (2020) 1098–1106.
[29] M. Roig-Oliver, P. Bresta, M. Nadal, G. Liakopoulos, D. Nikolopoulos, G. Karabourniotis, J. Bota, J. Flexas, Cell wall composition and thickness affect mesophyll conductance to CO_2 diffusion in *Helianthus annuus* under water deprivation, J. Exp. Bot. 71 (2020) 7198–7209.
[30] L. Sack, P.D. Cowan, N. Jaikumar, N.M. Holbrook, The 'hydrology' of leaves: coordination of structure and function intemperate woody species, Plant Cell Environ. 26 (2003) 1343–1356.
[31] Ü. Niinemets, Global-scale climatic controls of leaf dry mass per area, density, and thickness in trees and shrubs, Ecology 82 (2001) 453–469.
[32] J.P. Moore, J.M. Farrant, A. Driouich, A role for pectin-associated arabinans in maintaining the flexibility of the plant cell wall during water deficit stress, Plant Signal. Beh. 3 (2008) 102–104.
[33] D. Solecka, J. Zebrowski, A. Kacperska, Are pectins involved in cold acclimation and de-acclimation of winter oil-seed rape plants, Ann. Bot. 101 (2008) 521–530.
[34] T.E.G. Álvarez-Arenas, D. Sancho-Knapik, J.J. Peguero-Pina, A. Gómez-Arroyo, E. Gil-Pelegrín, Non-contact ultrasonic resonant spectroscopy resolves the elastic properties of layered plant tissues, Appl. Phys. Lett. 113 (2018), 253704.
[35] J. Miranda-Apodaca, U. Pérez-López, M. Lacuesta, A. Mena-Petite, A. Muñoz-Rueda, The interaction between drought and elevated CO_2 in water relations in two grassland species is species-specific, J. Plant Physiol. 220 (2018) 193–202.
[36] N.C. Carpita, D.M, D.M. Gibeaut, Structural models of primary cell walls in flowering plants: consistency of molecular structure with the physical properties of the walls during growth, Plant J. 3 (1993) 1–30.
[37] N.C. Carpita, M.C. McCann, The functions of cell wall polysaccharides in composition and architecture revealed through mutations, Plant Soil 247 (2002) 71–80.
[38] D.J. Cosgrove, Growth of the plant cell wall, Nat. Rev. Mol. Cell Biol. 6 (2005) 850–861.
[39] R. Tenhaken, Cell wall remodeling under abiotic stress, Front. Plant Sci. 5 (2015) 771.
[40] C.T. Anderson, J.J. Kieber, Dynamic construction, perception, and remodelling of plant cell walls, Ann. Rev. Plant Biol. 71 (2020) 39–69.
[41] M. Vicré, O. Lerouxel, J. Farrant, P. Lerouge, A. Driouich, Composition and desiccation-induced alterations of the cell wall in the resurrection plant *Craterostigma wilmsii*, Physiol. Plant. 120 (2004) 229–239.
[42] M.R. Leucci, M.S. Lenucci, G. Piro, G. Dalessandro, Water stress and cell wall polysaccharides in the apical root zone of wheat cultivars varying in drought tolerance, J. Plant Physiol. 165 (2008) 1168–1180.
[43] M.J. Clemente-Moreno, J. Gago, P. Díaz-Vivancos, A. Bernal, E. Miedes, P. Bresta, G. Liakopoulos, A.R. Fernie, J.A. Hernández, J. Flexas, The apoplastic antioxidant system and altered cell wall dynamics influence mesophyll conductance and the rate of photosynthesis, Plant J. 99 (2019) 1031–1046.
[44] J.L. Steiner, A.J. Flanzluebbers, Farming with grass – for people, for profit, for production, for protection, J. Soil Water Conserv. 64 (2009) 75A–80A.
[45] T.I. Odintsova, M.P. Slezina, E.A. Istomina, Defensins of grasses: a systematic review, Biomolecules 10 (2020) 1029.
[46] N.C. Carpita, Structure and biogenesis of the cell walls of grasses, Annu. Rev. Plant Physiol. Plant Mol. Biol. 47 (1996) 445–476.
[47] J. Vogel, J, Unique aspects of the grass cell wall, Curr. Opi. Plant Biol. 11 (2008) 301–307.
[48] R.D. Hatfield, D.M. Rancour, J.M. Marita, Grass cell walls: a story of cross-linking, Front. Plant Sci. 7 (2017) 2056.
[49] P.V. Ellsworth, P.Z. Ellsworth, N.K. Koteyeva, A.B. Cousins, Cell wall properties in *Oryza sativa* influence mesophyll CO_2 conductance, New Phytol. 219 (2018) 66–76.
[50] R. Valentini, D. Epron, P.D. Angelis, G. Matteucci, E. Dreyer, In situ estimation of net CO_2 assimilation, photosynthetic electron flow and photorespiration of Turkey oak (*Q. Cerris* L.) leaves: diurnal cycles under different water supply, Plant Cell Environ. 18 (1995) 631–664.
[51] Ü. Niinemets, A. Cescatti, M. Rodeghiero, T. Tosens, Leaf internal diffusion conductance limits photosynthesis more strongly in older leaves of Mediterranean evergreen broad-leaved species, Plant Cell Environ. 28 (2005) 1552–1566.
[52] P.C. Harley, F. Loreto, G. Di Marco, T.D. Sharkey, Theoretical considerations when estimating the mesophyll conductance to CO_2 flux by the analysis of the response of photosynthesis to CO_2, Plant Physiol. 98 (1992) 1429–1436.
[53] C. Hermida-Carrera, M.V. Kapralov, J. Galmés, Rubisco catalytic properties and temperature response in crops, Plant Physiol. 171 (2016) 2549–2561.
[54] L. Sack, J. Pasquet-Kok, Leaf pressure-volume curve parameters. Prometheus Wiki. Available at http://prometheuswiki.org/tiki-pagehistory.php?page=Leaf%20pressure-volume%20curve%20parameters&preview=16 (accessed 24 October 2020).
[55] M. Dubois, K.A. Gilles, J.K. Hamilton, P.A. Rebers, F. Smith F, Colorimetric method for determination of sugars and related substances, J. Anal. Chem. 28 (1956) 350–356.
[56] N. Blumenkrantz, G. Asboe-Hansen, New method for quantitative determination of uronic acids, Anal. Bioche. 54 (1973) 484–489.
[57] H. Medrano, J.M. Escalona, J. Bota, J. Gulías, J. Flexas, Regulation of photosynthesis of C_3 plants in response to progressive drought: stomatal conductance as a reference parameter, Ann. Bot. 89 (2002) 895–905.
[58] S. Salleo, M.A. Lo Gullo, Sclerophylly and plant water relations in three Mediterranean *Quercus* species, Ann. Bot. 65 (1990), 259–27.
[59] T. Saito, K. Soga, T. Hoson, I. Terashima, The bulk elastic modulus and the reversible properties of cell walls in developing *Quercus* leaves, Plant Cell Physiol. 47 (2006) 715–725.
[60] I.J. Wright, P.B. Reich, J.H.C. Cornelissen, D.S. Falster, P.K. Groom, K. Hikosaka, W. Lee, C.H. Lusk, Ü. Niinemets, J. Oleksyn, N. Osada, H. Poorter, D.I. Warton, M. Westoby, Modulation of leaf economic traits and trait relationships by climate, Glob. Ecol. Biogeogr. 14 (2005) 411–421.
[61] H. Poorter, Ü. Niinemets, L. Poorter, I.J. Wright, R. Villar, Causes and consequences of variation in leaf mass per area (LMA): a meta-analysis, New Phytol. 182 (2009) 565–588.
[62] M.T. Tyree, P.G. Jarvis P.G, Water in tissues and cells, in: O.L. Lange, P.S. Nobel, C. B. Osmond, H. Ziegler (Eds.), Physiological Plant Ecology II, Encyclopedia of Plant Physiology, Springer, Berlin, 1982, pp. 33–77.
[63] J.J. Peguero-Pina, D. Sancho-Knapik, E. Gil-Pelegrín, Ancient cell structural traits and photosynthesis in today's environment, J. Exp. Bot. 68 (2017) 1389–1392.
[64] J. Gago, D.M. Daloso, C.M. Figueroa, J. Flexas, A.R. Fernie, Z. Nikoloski Z, Relationships of leaf net photosynthesis, stomatal conductance, and mesophyll conductance to primary metabolism: a multispecies meta-analysis approach, Plant Physiol. 171 (2016) 265–279.
[65] L. Jones, J.L. Milne, D. Ashford, S.J. McQueen-Mason, S.J, Cell wall arabinan is essential for guard cell function, Proc. Natl. Acad. Sci. U.S.A. 100 (2003) 11783–11788.
[66] L. Jones, J.L. Milne, D. Ashford, M.C. McCann, S.J. McQueen-Mason, A conserved functional role of pectic polymers in stomatal guard cells from a range of plant species, Planta 221 (2005) 255–264.
[67] I. Shtein, Y. Shelef, Z. Marom, E. Zelinger, A. Schwartz, Z.A. Popper, B. Bar-On, S. Harpaz-Saad, Stomatal cell wall composition: distinctive structural patterns associated with different phylogenetic groups, Ann. Bot. 119 (2017) 1021–1033.
[68] M. Ye, Z. Zhang, G. Huang, Z. Xiong, S. Peng, Y. Li, Y, High leaf mass per area *Oryza* genotypes invest more leaf mass to cell wall and show a low mesophyll conductance, AoBP 12 (2020) plaa028.
[69] R. Zhang, H. Hu, Y. Wang, Z. Hu, S. Ren, J. Li, B. He, Y. Wang, T. Xia, P. Chen, G. Xie, L. Peng, A novel rice fragile *culm* 24 mutant encodes a UDP-glucose epimerase that affects cell wall property and photosynthesis, J. Exp. Bot. 71 (2020) 2956–2969.
[70] N. Carpita, D. Sabularse, D. Montezinos, D.P. Delmer, Determination of the pore size of cell walls of living plant cells, Science 205 (1979) 1144–1147.
[71] O. Baron-Epel, P.K. Gharyal, M. Schindler, Pectins as mediators of wall porosity in soybean cells, Planta 175 (1988) 389–395.
[72] L. Franková, S.C. Fry, Biochemistry and physiological roles of enzymes that 'cut and paste' plant cell-wall polysaccharides, J. Exp. Bot. 64 (2013) 3519–3550.